

TABLE II  
 ANGLES BETWEEN CRYSTALLOGRAPHIC PLANES FOR HEXAGONAL ELEMENTS

<i>HKiL</i>	<i>hkil</i>	Dy	Hf	Be	Gd	Y	Zr	
		<i>c/a</i>						
		1.5790	1.5822	1.5847	1.5870	1.5880	1.5893	
0001	10 $\bar{1}$ 8	12.839	12.864	12.884	12.902	12.910	12.920	
	10 $\bar{1}$ 7	14.599	14.628	14.650	14.670	14.679	14.690	
	10 $\bar{1}$ 6	16.903	16.935	16.960	16.984	16.994	17.007	
	10 $\bar{1}$ 5	20.035	20.072	20.101	20.128	20.140	20.155	
	10 $\bar{1}$ 4	24.504	24.548	24.582	24.614	24.627	24.645	
	20 $\bar{2}$ 7	27.517	27.564	27.601	27.635	27.650	27.670	
	10 $\bar{1}$ 3	31.289	31.341	31.381	31.418	31.434	31.455	
	20 $\bar{2}$ 5	36.104	36.159	36.202	36.242	36.259	36.281	
	10 $\bar{1}$ 2	42.353	42.411	42.456	42.498	42.516	42.539	
	20 $\bar{2}$ 3	50.556	50.613	50.657	50.698	50.716	50.739	
	10 $\bar{1}$ 1	61.257	61.306	61.344	61.379	61.394	61.414	
	20 $\bar{2}$ 1	74.665	74.694	74.717	74.738	74.748	74.759	
	10 $\bar{1}$ 0	90.000	90.000	90.000	90.000	90.000	90.000	
	21 $\bar{3}$ 2	21 $\bar{3}$ 2	67.481	67.522	67.554	67.583	67.596	67.613
		21 $\bar{3}$ 1	78.288	78.311	78.329	78.346	78.353	78.362
21 $\bar{3}$ 0		90.000	90.000	90.000	90.000	90.000	90.000	
11 $\bar{2}$ 8	11 $\bar{2}$ 8	21.542	21.581	21.612	21.641	21.653	21.669	
	11 $\bar{2}$ 6	27.759	27.807	27.845	27.879	27.894	27.913	
	11 $\bar{2}$ 4	38.291	38.348	38.392	38.432	38.450	38.472	
	11 $\bar{2}$ 2	57.653	57.706	57.747	57.784	57.800	57.822	
	11 $\bar{2}$ 0	90.000	90.000	90.000	90.000	90.000	90.000	
10 $\bar{1}$ 0	21 $\bar{3}$ 0	19.107	19.107	19.107	19.107	19.107	19.107	
	11 $\bar{2}$ 0	30.000	30.000	30.000	30.000	30.000	30.000	
	01 $\bar{1}$ 0	60.000	60.000	60.000	60.000	60.000	60.000	

7. KLEMM AND BOMMER, *Z. anorg. Chem.* **231**, 150 (1937).
8. SWANSON AND FUYAT, NBS Circular 539, Vol. III (1953).
9. KLEMM AND BOMMER, *Z. anorg. Chem.* **231**, 150 (1937).
10. QUILL, *Z. anorg. u. allgem. Chem.* **208**, 59 (1932).

R. E. FROUNFELKER  
 M. A. SEITZ  
 W. M. HIRTHE

Department of Mechanical Engineering  
 Marquette University  
 Milwaukee, Wisconsin

Received November 30, 1961

Revised July 18, 1962

## On the Possibility of Using Model Experiments to Study Shielding Problems

### The Method

It is a well-known fact that it is possible to study the penetration of gamma radiation theoretically only in the simplest cases. For more complicated configurations it is necessary to make full scale experiments which are both expensive and time consuming. One hitherto untried possi-

bility for simplifying the problem is to perform some kind of model experiment. The purpose of this paper is to discuss this method.

In the following we will deal with concrete shields. This is the case which has the greatest practical importance. In concrete the gamma radiation is attenuated almost entirely by Compton absorption, at least for those energies which are of interest in connection with shielding problems. An obvious way to decrease the dimensions of a shield is to increase the cross section of the Compton absorption by making the shield of some heavier element, for example, iron. Such an iron shield will constitute a good model of the concrete shield. It is evident, however, that a model experiment of this type gives no real gain. An iron shield having the same attenuation as a concrete shield is thinner but has the same weight and is more expensive.

The only possibility to decrease the size of the model further is to decrease the energy of the radiation source. In many practical shielding problems the gamma radiation of 6-8 Mev energy has maximum penetrability and hence it determines the dimensions of the shield. If it is possible to make a model experiment using a radiation source emitting 2-3 Mev gamma radiation, it would be of great importance. An iron model of a thick concrete shield would then be of a reasonable size. Furthermore, there is the great advantage that one is not limited to work with a reactor or an accel-

erator, but one can perform shielding experiments with cheap and handy radioactive sources.

The question now is to what extent a shielding experiment performed at low energy is a model of an experiment at high energy. It is easy to give the conditions for a perfect model experiment. We consider the scattering of a photon at a certain angle for two different initial energies. The first condition is that the ratio of the differential cross sections at the two energies is independent of the scattering angle. This condition is not well fulfilled. When the energy of the initial photons is increased, the scattered photons will be more concentrated in the forward direction. However, the deviations are not too serious for higher energies (over 1 Mev) and for small scattering angles. The second condition is that the cross section increases with decreasing energy in such a way that the cross sections for the two scattered photons have the same ratio as the cross sections of the two initial photons. This second condition is also not fulfilled. The increase of the Compton cross section is not rapid enough for lower energies. It is interesting to note, however, that the deviations from these two conditions partly cancel. When the energy decreases, the relative intensity in the forward direction decreases but at the same time there is a relative increase of the penetrability of the photons.

Hence this discussion indicates that a model experiment might work at high energies but that it certainly breaks down for low energies. When a photon has been scattered several times and has lost most of its energy, the remaining energy is almost independent of the initial energy. The same is true when a photon makes a large angle scattering and loses most of its energy in a single collision. This fact is perhaps not too serious for the model experiment for the following reason. When a photon has lost most of its energy, the probability of it penetrating further through the shield is small. Hence the low energy photons which emerge from a shield must have come down in the low energy region not too far from the surface of the shield. This means that the deviation of the model experiment from the full-scale experiment should be limited mainly to the surface layer of the shield and, hence, might not be too disturbing.

There is another reason that a model experiment should be more useful than one might think at first. It is certainly true that a model is such a poor approximation of a full scale shield that it never can be used to determine, for example, energy spectra of the penetrating radiation or buildup factors. However, if one limits the model experiments to relative intensities only, it should be considerably more accurate. An important application would be, for example, a shield having ducts or holes through it. Even if there are considerable deviations in a model experiment, these deviations should be approximately the same all over the shield. Hence a model might be useful for determining the relative intensities. The restriction to relative values is not a serious disadvantage since the absolute attenuation of bulk shields is very well-known, both experimentally and theoretically (*t*).

In order to decide about the feasibility of model experiments a quantitative analysis is necessary. Calculations on the penetration of gamma radiation are extremely difficult except for very simple geometries; consequently, some experiments, which are described in the next section, have been performed.

#### Experiment

In this experiment the penetration of 7 Mev gamma radiation through a concrete shield was compared with the penetration through an iron model. A schematic picture of the experimental arrangement for the full scale experiment is shown in Fig. 1. The concrete shield was built up of big concrete blocks. It had a thickness of 70 cm, a height of 250 cm, and a length of 300 cm. In some of the experiments the shield had holes of different types. In Fig. 1 is shown the case of a straight hole. The source of the gamma radiation was a 4 Mev v. d. G. generator producing 7 Mev gamma rays in the reaction  $F^{19}(p, \alpha\gamma)O^{16}$ . The beam tube was 1300 cm above the floor, running parallel to the surface of the shield at a distance of 35 cm. The intensity of the transmitted radiation was measured by means of a scintillation spectrometer having a  $1\frac{1}{2}$  in.  $\times$  2 in. sodium iodide crystal. The crystal was at a distance of 5 cm from the shield in all experiments except one, in which the distance was 20 cm. The spectrometer was movable along a vertical line perpendicular to the normal through the radiation source. The position of the spectrometer was measured from the normal (distance *X* in Fig. 1). The pulses from the scintillation spectrometer were analyzed by a single channel pulse height analyzer so that it was possible to select pulses corresponding to a certain energy interval in the spectrum of the transmitted radiation. The width of the interval was about 30% of the mean energy. For an accurate determination of the spectrum shape, which is important in the interpretation of the data, a 4 in.  $\times$  5 in. sodium iodide crystal was used.

The radiation source in the model experiment should have an energy between 2 and 3 Mev. Furthermore, it should be monoenergetic and not too short-lived. These requirements are met fairly well by RdTh, which emits gamma radiation with an energy of 2.62 Mev. Some other gamma rays are also emitted but their energy is low and hence they are so easily absorbed that they do not disturb the measurements.

The model was made of iron in the scale 1:5.6. The scale factor was determined by the densities of concrete and iron and by the ratio between the Compton cross sections at 7 Mev and 2.62 Mev. The thickness of the iron shield then becomes 12.5 cm. It was built up of a number of iron pieces

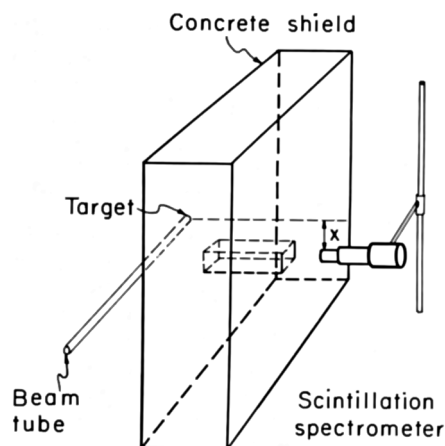


FIG. 1. A schematic picture of the experimental arrangement in the full scale experiment.

and was very easy to handle. The holes in the shield and the distances of the source and the crystal from the shield were also scaled down by the same factor. In the model experiment the radiation intensity was also determined by a scintillation spectrometer but the crystal size was now  $\frac{1}{2}$  in.  $\times$   $\frac{1}{2}$  in. This size was a result of a compromise between two opposite tendencies. It is desirable to have a small crystal in order to get a good spatial resolution but, on the other hand, the crystal should be big in order to make it easier to select a certain part of the gamma spectrum without interference from other parts of the spectrum.

In the full scale experiment the intensity distribution was measured along the surface of the shield for a number of gamma energy intervals. It is then necessary to know the energy values of the corresponding intervals in the model experiment. An analysis shows that there is a correspondence between the energy values in the two spectra. To a certain energy value in the 7 Mev experiment corresponds an energy value in the 2.6 Mev experiment, which is reached by the same sequence of collisions. It turns out that this latter value does not depend very much on how the energy decrease has taken place; for example, whether it has occurred in one single collision with a large deflection or in many small angle collisions. Hence, to a certain energy range in the full scale experiment corresponds a well-defined energy range in the model experiment. Its energy value is calculated by assuming a single collision with the same deflection in the two cases. The deflection angle is, of

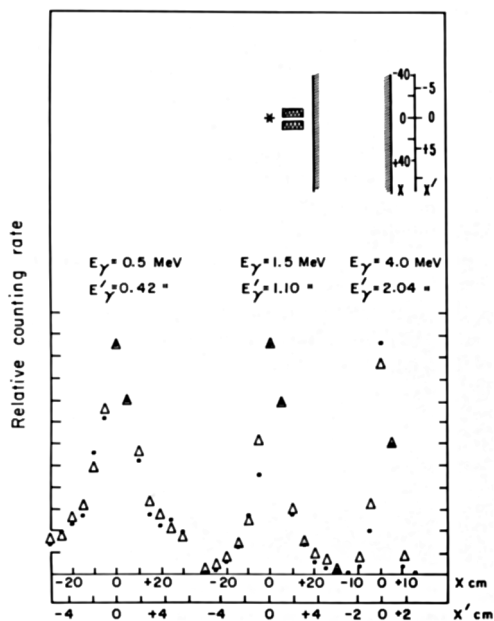


Fig. 2. Collimated radiation incident upon a bulk shield. The experimental arrangement is shown in the inset. The  $X$  scale, which indicates the position of the spectrometer, refers to the full scale experiment, the  $X'$  scale to the model experiment. The selected energies in the full scale experiment  $E_\gamma$ , and in the model experiment  $E_\gamma'$  are shown for each distribution. Dots: measured values in the full scale experiment; triangles: values in the model experiment. The measured values are normalized so that the area under a curve in the full scale experiment is the same as the area under the corresponding model curve.

course, defined by the selected energy value in the full scale experiment. We can, for example, consider an energy interval around 1.5 Mev in the full scale experiment. The energy change from 7 Mev to 1.5 Mev can be obtained in a single collision with a deflection angle of  $42^\circ$ . The same collision in the model experiment will change the energy from 2.62 Mev to 1.10 Mev. Hence the energy 1.10 Mev in the model experiment corresponds to the energy 1.50 Mev in the full scale experiment.

In connection with the use of the scintillation spectrometer it is necessary to pay some attention to the response function of the spectrometer. It is usually difficult to pick out a narrow energy band in a continuous spectrum since the Compton distribution of the radiation having a greater energy than the selected one will disturb the measurements. In the present case this complication is of less importance because of the fact that the spectrum of the secondary radiation from the shield falls off rapidly with increasing energy. Another helpful circumstance is that the efficiency of the crystal decreases with increasing energy.

Figure 2 shows the result of an experiment in which the incident radiation was strongly collimated. The insert shows the experimental arrangement. The radiation intensity was measured along a line perpendicular to the symmetry axis. The distance between the crystal and the shield was 5 cm in the full scale experiment and 2 mm in the model experiment. In this figure, as well as in the following ones, the dots denote values obtained in the full scale experiment and triangles values from the model experiment. The measured quantity is the number of pulses per second. From this it is possible to calculate the photon flux and the dose. However, since we are only interested in relative values the measured distributions are compared directly. The ordinate scales are adjusted so that the two distributions get the same area.

The results in Fig. 2 are very easy to interpret. When the energy of the selected energy interval increases, the distribution becomes narrower. This, of course, is due to the fact that a high secondary energy means that the photons could not have suffered any large angle deflection, but that they proceed almost in the original direction. The main result of this experiment is that the agreement between model experiment and full scale experiment is remarkably good. This experiment gives a measure of the change of direction of the photons. Hence the model experiment seems to work well in this important respect.

Figure 3 shows the penetration through a shield, which has a straight hole to the side of the radiation source as indicated in the insert. The relative position of the source, the hole, and the spectrometer is shown in the figure, which is drawn to scale. The measurements were made as in the previous case. For high secondary energies the preceding experiment shows that the change of direction is small. Hence the penetration is mainly determined by the amount of matter along the line joining the radiation source and the crystal. The maximum of the intensity distribution should therefore come somewhat below the position of the hole. This is indeed the case. When the energy of the measured radiation is decreased, an interesting effect occurs. The maximum of the curve is shifted and for a secondary energy of 0.25 Mev it comes right at the hole. This shows that a stream of low energy photons comes through the hole. A direct measurement of the shape of the energy spectrum showed also a great excess of low energy photons in front

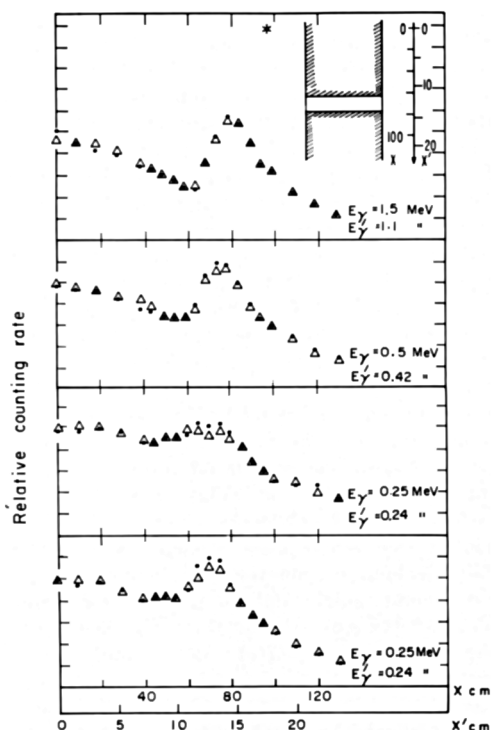


FIG. 3. Shield with a straight hole. The cross section of the hole is  $17 \times 17$  cm. The relative position of the gamma-ray source, the shield, and the spectrometer is drawn to scale in the insert. The notation is the same as in Fig. 2. The second curve from the bottom was obtained with a crystal-shield distance of 20 cm. For all other curves this distance was 5 cm.

of the hole. The reason for this is obvious; there occurs a kind of diffusion of low energy radiation through the hole.

It will be noted that the agreement between the model experiment and the full scale experiment is good also in this rather complicated geometry. The only systematic deviation is that the peak value is somewhat too low in the model experiment for the 0.25 Mev interval. This might be due to the fact that the photoelectric absorption is relatively greater in iron than in concrete. The low energy photons which diffuse through the hole are partly absorbed in the regions of the shield which surround the hole. This absorption will be too strong in the model experiment. This effect is small, however, and a careful study of this problem might make it possible to apply a correction.

With this geometry an experiment was made in which the distance between crystal and shield was 20 cm. Good agreement was also obtained in this case.

In Fig. 4 are shown the results of an experiment with an even more complicated arrangement: a shield with a hole having two bends. This configuration is essentially a combination of the first two, with the first leg of the duct serving as the collimator. It is interesting to note that in this case the curves for different secondary energies are very similar. There are no greater amounts of low energy photons coming through the hole. The peak, which has the position corresponding to the opening of the hole, increases slightly with decreasing energy but the effect is rather insignificant. This

indicates that a bend is an efficient way of stopping the diffusion of gamma radiation through a hole. Also in this case the model experiment agrees very well with the full scale experiment.

The present experiment gives the intensity distributions as number of photons per second in a certain energy range. This quantity has the greatest physical significance but in practice one is usually more interested in the total dose. It can be calculated fairly easily from the measured values since the energy distributions are well-known both theoretically and experimentally (1).

It is interesting to note that the low energy photons give a relatively smaller contribution to the dose than the high energy ones. As discussed above, the model experiment works best for the high energy photons. Hence the accuracy of this model technique will be greater when the intensity is expressed as a dose rate than when it is expressed as number of photons per sec.

The experiments reported in the present paper have used 7 Mev gamma rays as the radiation source in the full scale experiment. The reason is that, using a v. d. G. generator, any other sources of monoenergetic gamma radiation having sufficient intensity are unavailable. An important question is how well the model technique works at other energies. For lower energies there should be no problems since the full scale experiment and the model experiment became more similar when the energy difference between the sources decreases. For higher energies an increase to 10-15 Mev is not expected to cause any basic changes and most sources of interest in shielding problems fall below this limit. For still higher energies, however, special problems may arise, especially when pair production begins to become important.

In the present work we have limited ourselves to point

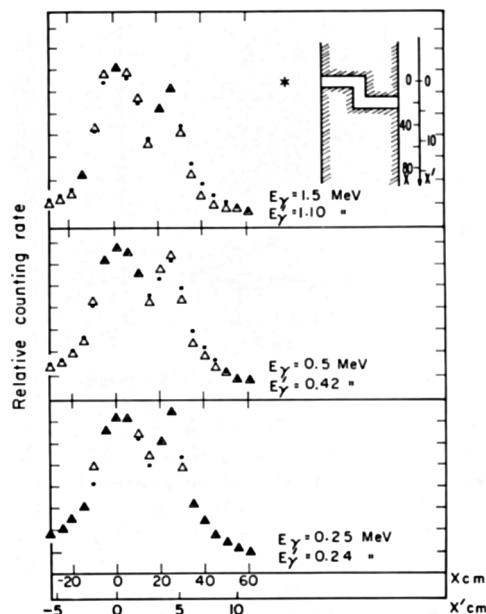


FIG. 4. Shield with a hole having an offset. The cross section of the hole is: height 11 cm, width, 17 cm. The offset is 20 cm. The relative position of the gamma-ray source, the shield, and the spectrometer is drawn to scale in the insert. The notation is the same as in Fig. 2.

sources. It is, of course, easy to modify the model experiment in the case of extended sources. One can, for example, use radioactive solutions as sources.

Another limitation is the use of monoenergetic radiation. In most practical applications the radiation source has a continuous spectrum. The dimensions of a shield are determined by those gamma rays which have a high penetrability as well as a high intensity. Knowing the energy spectrum of the source and the cross section curve one can easily find out the energy range of the primary radiation which gives the main contribution to the dose. In many cases it turns out that this energy range is so narrow that the source can be regarded as semimonoenergetic. The technique will then be exactly the same as described here. If this is not possible one can always divide the energy spectrum of the radiation source in a number of intervals and perform an experiment for each interval.

#### Discussion

It would be especially interesting to study the present problem from a theoretical point of view. However, most cases of practical interest are too complicated to allow a theoretical calculation of the gamma penetration. The studies, which exist for simple geometries, do not give any information of interest for the present discussion. However, a recent work by Leimdörfer (2) is of very great interest here. This calculation corresponds to the first of the three cases described above, namely, a collimated beam incident upon a shield. The input parameters were chosen to be the

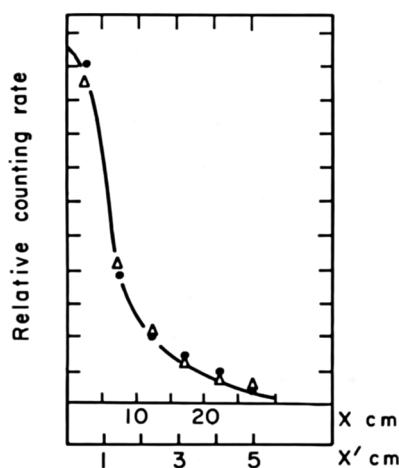


FIG. 5. A comparison between theoretical and experimental intensity distributions of the transmitted radiation with the incident radiation well collimated. The curve in the figure is the experimental shape of the distribution for an energy of 1.5 Mev in the full scale experiment and 1.1 Mev in the model experiment. This curve is the best fit to the experimental points in the middle of Fig. 2. The theoretical values are the calculated counting rates derived from the work of Leimdörfer for the same energies. Dots: theoretical values for 7 Mev radiation incident upon a concrete shield (corresponding to the full scale experiment); triangles: 2.62 Mev radiation incident upon an iron shield (corresponding to the model experiment). The  $X$  scale refers to the full scale experiment, the  $X'$  scale to the model experiment.

same as in the present experiments. The geometry used was that of a narrow beam of gamma radiation impinging at an arbitrary angle on the surface of a one-medium slab of finite thickness and infinite extension. The output contains the following information: Reflected and transmitted (differential) current and flux, distributed into arbitrarily chosen bins in energy, angle, and radius of exit. The code works with statistical weights and all calculated quantities are accompanied by error estimates. Histories are terminated either by the passage of a preset minimum weight or energy limit. Pair production processes may be succeeded by the isotropic birth of a doubly weighted annihilation quantum. Sampling from the Klein-Nishina formula is performed according to the approximation given in ref. 3. The energy region presently covered is 10 Mev-10 kev.

Two conclusions can immediately be drawn from the preliminary results of the calculation. First, there is good agreement between the calculated intensities and corresponding experimental values. This shows that the Monte Carlo code describes very well the penetration of the gamma radiation. In the second place, a comparison can be made between the calculated penetration of 7 Mev gamma radiation in a concrete shield and 2.6 Mev gamma radiation in an iron shield. It turns out that the intensity distributions after the penetration of the shield are similar in the two cases if the comparison is made for energy intervals whose energy is related in the way discussed above in connection with the experimental work. This fact lends strong support to the feasibility of using the model technique described here.

An example of the results of the theoretical calculations is shown in Fig. 5. The curve gives the experimental distribution for a secondary energy of 1.5 Mev in the full scale experiment (1.1 Mev in the model experiment). This curve is the best fit to the experimental points in Fig. 2. The theoretical results are shown in Fig. 5 as dots (7 Mev, concrete) and triangles (2.6 Mev, iron). The agreement is quite good. When more extensive theoretical results become available, a more detailed analysis can be made.

In the present work the interest has been limited to full scale shields of concrete. Obviously the same method can be used for shields of other light materials, for example, water.

There should be numerous shielding problems in which the model technique described here might be useful. Reactor shields offer many interesting applications, especially the case of holes and ducts. Another problem of great importance is the shielding of high energy electron accelerators, which are used more and more in technical and medical applications. A third case, which might be mentioned, is the civil defense against atomic weapons. It might be possible to study the design of shelters by means of the model technique.

If a shielding problem can be studied by model experiments it means several advantages. The work can be done without access to accelerators or reactors. The experimental work becomes very much simpler. With a number of iron pieces one can easily build up and study models of different types. The effect of changes in a certain shield can be investigated very easily. Hence, by trial and error one can find the solution to problems which might be difficult to study in other ways.

The results obtained in the present investigation indicate that the model technique gives quite accurate results and

that it should be quite useful in several cases. However, it is clearly necessary to do further work in order to find out the limitations of this method. It would be desirable to study a greater variety of geometries as well as investigating the theoretical aspects of the problem more in detail.

The author is greatly indebted to Mr. M. Leimdörfer, A. B. Atomenergi, Stockholm, for communicating his results prior to publication and for interesting discussion.

## REFERENCES

1. H. GOLDSTEIN, "Fundamental Aspects of Reactor Shielding." Addison-Wesley, Reading, Massachusetts, 1959.
2. M. LEIMDÖRFER, to be published.
3. B. CARLSON, The Monte Carlo method applied to a problem in  $\gamma$ -ray diffusion. AECU-2857 (1953).

SVEN A. E. JOHANSSON

Department of Physics  
University of Lund  
Lund, Sweden

Received December 27, 1961

Revised July 12, 1962

## Two Regimes of Burnout (DNB) Correlated with Steam Energy Flow for Uniformly-Heated Channels

Experimental determinations of "burnout heat flux" in subcooled or boiling-water systems have generally been supplanted by measurements which determine the heat flux at which nucleate boiling has become intense enough to start formation of a low-conductivity film of steam on the surface. The phenomenon is frequently called "departure from nucleate boiling" (DNB), and is usually considered to occur at heat fluxes only a few percent below those causing physical burnout and destruction of the test element. When published values of DNB heat-flux are plotted against such arguments as quality ( $x$ ), enthalpy ( $h$ ), or mass velocity ( $G$ ) the data show wide scatter.

This scatter is minimized when the data are plotted against the argument  $G(h - h_{\text{saturation}})$ , which has the same dimensions as heat flux, Btu/ft<sup>2</sup> hr or watts/cm<sup>2</sup>. In a boiling channel  $G(h - h_f)$  can be called "steam energy flow" or "SEF" and signifies the rate of flow of enthalpy of vaporization across unit flow area. Its value at the core exit is a measure of boiling reactor performance, and depends only upon the flow of feedwater which is totally vaporized in the core, not upon any accompanying recirculating saturated-water flow used as a "carrier" for the feedwater.

$G(h - h_{fg})$  has a negative value for subcooled water, and is a convenient correlating parameter in the subcooled region also. The use of negative values of steam energy flow is analogous to the use of "negative quality" ( $x < 0$ ) in other correlations.

Figure 1 is a typical plot of DNB heat flux against SEF with uniform axial power distribution. Two distinct regimes of DNB exist. The upper (DNB-1) regime shows continuously decreasing DNB heat flux with increasing SEF

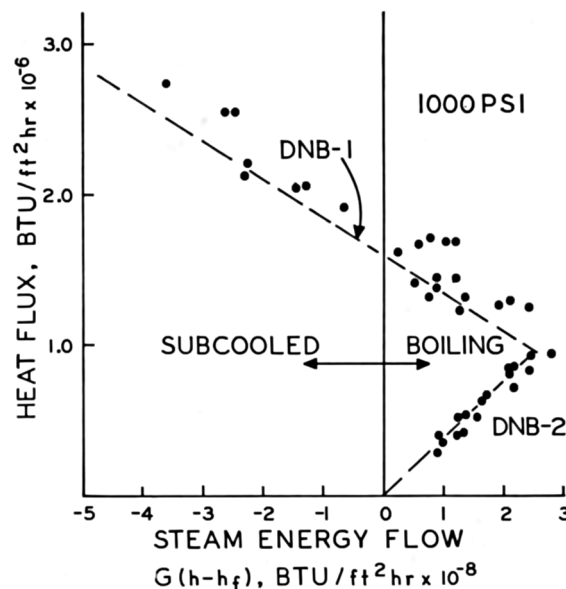


FIG. 1. DNB heat flux vs. steam energy flow at 1000 psi in vertical tubes. Data from WAPD-188 and ANL4627.

through the subcooled region and extending well into the quality region. In this regime the transition from normal boiling into film blanketing is usually a sharp one, and usually occurs at heat fluxes exceeding  $0.5 \times 10^6$  Btu/ft<sup>2</sup> hr. Burnout of this type can be considered a *thermal instability*.

A lower-heat-flux (DNB-2) regime exists in channels with net boiling. The data plot along a line which corresponds to a constant ratio of boiling length to thermal equivalent diameter,  $L_B/D_Q = (Q/A)/4G(h - h_f)$  and consequently to a constant ratio of boiling length to total length  $L_B/L_T$ . The thermal equivalent diameter,  $D_Q = 4$  (flow area)/(heated perimeter) is identical to hydraulic diameter when heated and wetted perimeters are identical. Usually,

$$0.8 \leq (L_B/L_T)_{\text{DNB-2}} \leq 1.0 \quad (1)$$

Equation (1) signifies that most data obtained with the boiling length greater than 80% of the total length lie in the DNB-2 regime. DNB in this regime has been observed at heat fluxes as low as  $10^4$  Btu/ft<sup>2</sup> hr; it is usually accompanied by large oscillations in flow and pressure drop and can be considered a *hydrodynamic instability*.

In each regime high-quality, low-mass-velocity points lie adjacent to low-quality, high-mass-velocity points.

For data in which  $L_B/L_T < (L_B/L_T)_{\text{DNB-2}}$ , hydrodynamic instabilities are seldom found and points lie in the DNB-1 regime. A simple expression which describes the major trends in DNB-1 data over wide ranges of subcooled and quality operation is:

$$(Q/A)_{\text{DNB-1}} = [(Q/A)_{\text{DNB-1}}]_{h=h_f} - \frac{G(h - h_f)}{A} \quad (2)$$

To fit data considered here, substitution of empirical constants provides (2a) in the Btu-ft-hr-lb system.

$$(Q/A)_{\text{DNB-1}} = 3.8(h_{fg})^2 - \frac{G(h - h_f)}{400} \quad (2a)$$

$$14.7 \text{ psi} \leq P \leq 2750 \text{ psi.}$$